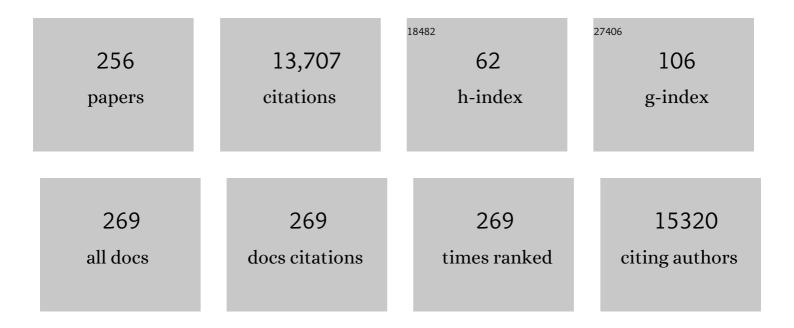
Vincent A Magnotta

List of Publications by Year in descending order

Source: https://exaly.com/author-pdf/1743908/publications.pdf Version: 2024-02-01



#	Article	IF	CITATIONS
1	Long-term Antipsychotic Treatment and Brain Volumes. Archives of General Psychiatry, 2011, 68, 128.	12.3	871
2	Widespread white matter microstructural differences in schizophrenia across 4322 individuals: results from the ENIGMA Schizophrenia DTI Working Group. Molecular Psychiatry, 2018, 23, 1261-1269.	7.9	522
3	Progressive Structural Brain Abnormalities and Their Relationship to Clinical Outcome. Archives of General Psychiatry, 2003, 60, 585.	12.3	501
4	Progressive Brain Change in Schizophrenia: A Prospective Longitudinal Study of First-Episode Schizophrenia. Biological Psychiatry, 2011, 70, 672-679.	1.3	320
5	Structural MR image processing using the brains2 toolbox. Computerized Medical Imaging and Graphics, 2002, 26, 251-264.	5.8	297
6	The Neurodevelopmental Impact of Childhood-onset Temporal Lobe Epilepsy on Brain Structure and Function. Epilepsia, 2002, 43, 1062-1071.	5.1	252
7	Improving Tissue Classification in MRI: A Three-Dimensional Multispectral Discriminant Analysis Method with Automated Training Class Selection. Journal of Computer Assisted Tomography, 1999, 23, 144-154.	0.9	232
8	Longitudinal change in regional brain volumes in prodromal Huntington disease. Journal of Neurology, Neurosurgery and Psychiatry, 2011, 82, 405-410.	1.9	220
9	Striatal and white matter predictors of estimated diagnosis for Huntington disease. Brain Research Bulletin, 2010, 82, 201-207.	3.0	214
10	Brain Structure in Preclinical Huntington's Disease. Biological Psychiatry, 2006, 59, 57-63.	1.3	208
11	Tumor perfusion studies using fast magnetic resonance imaging technique in advanced cervical cancer: A new noninvasive predictive assay. International Journal of Radiation Oncology Biology Physics, 1996, 36, 623-633.	0.8	202
12	Gyrification abnormalities in childhood- and adolescent-onset schizophrenia. Biological Psychiatry, 2003, 54, 418-426.	1.3	185
13	Insular cortex abnormalities in schizophrenia: a structural magnetic resonance imaging study of first-episode patients. Schizophrenia Research, 2000, 46, 35-43.	2.0	182
14	Phase I/II randomized trial of aerobic exercise in Parkinson disease in a community setting. Neurology, 2014, 83, 413-425.	1.1	180
15	Measurement of Brain Structures with Artificial Neural Networks: Two- and Three-dimensional Applications. Radiology, 1999, 211, 781-790.	7.3	177
16	The MCIC Collection: A Shared Repository of Multi-Modal, Multi-Site Brain Image Data from a Clinical Investigation of Schizophrenia. Neuroinformatics, 2013, 11, 367-388.	2.8	168
17	Registration and machine learning-based automated segmentation of subcortical and cerebellar brain structures. Neurolmage, 2008, 39, 238-247.	4.2	155
18	An MRI-Based Parcellation Method for the Temporal Lobe. NeuroImage, 2000, 11, 271-288.	4.2	154

#	Article	IF	CITATIONS
19	Reducing inter-scanner variability of activation in a multicenter fMRI study: Role of smoothness equalization. NeuroImage, 2006, 32, 1656-1668.	4.2	148
20	Reduced cerebellar volume and neurological soft signs in first-episode schizophrenia. Psychiatry Research - Neuroimaging, 2005, 140, 239-250.	1.8	145
21	A new method for the in vivo volumetric measurement of the human hippocampus with high neuroanatomical accuracy. Hippocampus, 2000, 10, 752-758.	1.9	144
22	Pixel analysis of MR perfusion imaging in predicting radiation therapy outcome in cervical cancer. Journal of Magnetic Resonance Imaging, 2000, 12, 1027-1033.	3.4	143
23	Cerebral cortex structure in prodromal Huntington disease. Neurobiology of Disease, 2010, 40, 544-554.	4.4	142
24	Measurement of Signal-to-Noise and Contrast-to-Noise in the fBIRN Multicenter Imaging Study. Journal of Digital Imaging, 2006, 19, 140-147.	2.9	140
25	Early Change in Ferumoxytol-Enhanced Magnetic Resonance Imaging Signal Suggests Unstable Human Cerebral Aneurysm. Stroke, 2012, 43, 3258-3265.	2.0	138
26	Anatomic and Functional Variability: The Effects of Filter Size in Group fMRI Data Analysis. NeuroImage, 2001, 13, 577-588.	4.2	136
27	White Matter Abnormalities in Veterans With Mild Traumatic Brain Injury. American Journal of Psychiatry, 2012, 169, 1284-1291.	7.2	136
28	Detecting activity-evoked pH changes in human brain. Proceedings of the National Academy of Sciences of the United States of America, 2012, 109, 8270-8273.	7.1	134
29	Abnormal Brain Structure in Children With Isolated Clefts of the Lip or Palate. JAMA Pediatrics, 2007, 161, 753.	3.0	133
30	Effects of olanzapine on cerebellar functional connectivity in schizophrenia measured by fMRI during a simple motor task. Psychological Medicine, 2001, 31, 1065-1078.	4.5	130
31	Human Frontal Cortex: An MRI-Based Parcellation Method. NeuroImage, 1999, 10, 500-519.	4.2	122
32	Regional frontal abnormalities in schizophrenia: a quantitative gray matter volume and cortical surface size study. Biological Psychiatry, 2000, 48, 110-119.	1.3	121
33	Smaller intracranial volume in prodromal Huntington's disease: evidence for abnormal neurodevelopment. Brain, 2011, 134, 137-142.	7.6	118
34	Voxel-based Morphometric Multisite Collaborative Study on Schizophrenia. Schizophrenia Bulletin, 2009, 35, 82-95.	4.3	117
35	Proton echoâ€planar spectroscopic imaging of <i>J</i> â€coupled resonances in human brain at 3 and 4 Tesla. Magnetic Resonance in Medicine, 2007, 58, 236-244.	3.0	115
36	Evidence That Acetylsalicylic Acid Attenuates Inflammation in the Walls of Human Cerebral Aneurysms: Preliminary Results. Journal of the American Heart Association, 2013, 2, e000019.	3.7	115

#	Article	IF	CITATIONS
37	Multi-shot sensitivity-encoded diffusion data recovery using structured low-rank matrix completion (MUSSELS). Magnetic Resonance in Medicine, 2017, 78, 494-507.	3.0	115
38	Global White Matter Abnormalities in Schizophrenia: A Multisite Diffusion Tensor Imaging Study. Schizophrenia Bulletin, 2011, 37, 222-232.	4.3	113
39	Long-term Outcome of Brain Structure in Premature Infants. JAMA Pediatrics, 2011, 165, 443-50.	3.0	106
40	Usefulness of tumor volumetry by magnetic resonance imaging in assessing response to radiation therapy in carcinoma of the uterine cervix. International Journal of Radiation Oncology Biology Physics, 1996, 35, 915-924.	0.8	105
41	Hippocampal Volume and Mood Disorders After Traumatic Brain Injury. Biological Psychiatry, 2007, 62, 332-338.	1.3	104
42	Macrophage Imaging Within Human Cerebral Aneurysms Wall Using Ferumoxytol-Enhanced MRI: A Pilot Study. Arteriosclerosis, Thrombosis, and Vascular Biology, 2012, 32, 1032-1038.	2.4	98
43	Hippocampal volume and 2-year outcome in depression. British Journal of Psychiatry, 2008, 192, 472-473.	2.8	97
44	Tumor size evaluated by pelvic examination compared with 3-D MR quantitative analysis in the prediction of outcome for cervical cancer. International Journal of Radiation Oncology Biology Physics, 1997, 39, 395-404.	0.8	95
45	MR microcirculation assessment in cervical cancer: Correlations with histomorphological tumor markers and clinical outcome. Journal of Magnetic Resonance Imaging, 1999, 10, 267-276.	3.4	93
46	Predicting Control of Primary Tumor and Survival by DCE MRI During Early Therapy in Cervical Cancer. Investigative Radiology, 2009, 44, 343-350.	6.2	91
47	A Review of Challenges in the Use of fMRI for Disease Classification / Characterization and A Projection Pursuit Application from A Multi-site fMRI Schizophrenia Study. Brain Imaging and Behavior, 2008, 2, 207-226.	2.1	89
48	The Acute Effects of Aerobic Exercise onÂthe Functional Connectivity of Human Brain Networks. Brain Plasticity, 2017, 2, 171-190.	3.5	88
49	Extratemporal quantitative MR volumetrics and neuropsychological status in temporal lobe epilepsy. Journal of the International Neuropsychological Society, 2003, 9, 353-362.	1.8	85
50	Hippocampal volume in chronic posttraumatic stress disorder (PTSD): MRI study using two different evaluation methods. Journal of Affective Disorders, 2006, 94, 121-126.	4.1	84
51	Morphology of the ventral frontal cortex in schizophrenia: relationship with social dysfunction. Biological Psychiatry, 2002, 52, 1-8.	1.3	78
52	Morphology of the Cerebral Cortex in Preclinical Huntington's Disease. American Journal of Psychiatry, 2007, 164, 1428-1434.	7.2	78
53	IA-FEMesh: An open-source, interactive, multiblock approach to anatomic finite element model development. Computer Methods and Programs in Biomedicine, 2009, 94, 96-107.	4.7	78
54	MultiCenter Reliability of Diffusion Tensor Imaging. Brain Connectivity, 2012, 2, 345-355.	1.7	77

#	Article	IF	CITATIONS
55	Fully automated analysis using BRAINS: AutoWorkup. NeuroImage, 2011, 54, 328-336.	4.2	76
56	Prediction of tumor control in patients with cervical cancer: analysis of combined volume and dynamic enhancement pattern by MR imaging American Journal of Roentgenology, 1998, 170, 177-182.	2.2	74
57	Global and regional cortical thinning in first-episode psychosis patients: relationships with clinical and cognitive features. Psychological Medicine, 2011, 41, 1449-1460.	4.5	72
58	Abnormal brain development in child and adolescent carriers of mutant huntingtin. Neurology, 2019, 93, e1021-e1030.	1.1	72
59	Manual and Semiautomated Measurement of Cerebellar Subregions on MR Images. NeuroImage, 2002, 17, 61-76.	4.2	70
60	Marijuana alters the human cerebellar clock. NeuroReport, 2003, 14, 1145-1151.	1.2	70
61	Altered white matter microstructural organization in posttraumatic stress disorder across 3047 adults: results from the PGC-ENIGMA PTSD consortium. Molecular Psychiatry, 2021, 26, 4315-4330.	7.9	69
62	Hippocampal volume in first episode and recurrent depression. Psychiatry Research - Neuroimaging, 2009, 174, 62-66.	1.8	68
63	Cerebral cortex: a topographic segmentation method using magnetic resonance imaging. Psychiatry Research - Neuroimaging, 2000, 100, 97-126.	1.8	66
64	Reduced thalamic volume in first-episode non-affective psychosis: Correlations with clinical variables, symptomatology and cognitive functioning. NeuroImage, 2007, 35, 1613-1623.	4.2	66
65	Serial Therapy-Induced Changes in Tumor Shape in Cervical Cancer and Their Impact on Assessing Tumor Volume and Treatment Response. American Journal of Roentgenology, 2006, 187, 65-72.	2.2	64
66	Brain abnormalities in bipolar disorder detected by quantitative T1ϕmapping. Molecular Psychiatry, 2015, 20, 201-206.	7.9	61
67	Validating an image-based fNIRS approach with fMRI and a working memory task. NeuroImage, 2017, 147, 204-218.	4.2	61
68	Acute Exercise Effects Predict Training Change in Cognition and Connectivity. Medicine and Science in Sports and Exercise, 2020, 52, 131-140.	0.4	61
69	Neurodevelopmental vulnerability of the corpus callosum to childhood onset localization-related epilepsyâ~†â~†Supported in part by NIH Grants NS R01-37738 and MO1-RR03186 NeuroImage, 2003, 18, 284-29	92 <mark>4</mark> .2	60
70	Peripheral inflammation during abnormal mood states in bipolar I disorder. Journal of Affective Disorders, 2015, 187, 172-178.	4.1	60
71	Selective reduction of the posterior superior vermis in men with chronic schizophrenia. Schizophrenia Research, 2002, 55, 61-67.	2.0	59
72	Regionally selective atrophy of subcortical structures in prodromal HD as revealed by statistical shape analysis. Human Brain Mapping, 2014, 35, 792-809.	3.6	58

#	Article	IF	CITATIONS
73	Manual and Automated Measurement of the Whole Thalamus and Mediodorsal Nucleus Using Magnetic Resonance Imaging. NeuroImage, 2002, 17, 631-642.	4.2	54
74	Evaluation of the GTRACT diffusion tensor tractography algorithm: A validation and reliability study. NeuroImage, 2006, 31, 1075-1085.	4.2	53
75	Metabolic Correlates of Antidepressant and Antipsychotic Response in Patients With Psychotic Depression Undergoing Electroconvulsive Therapy. Journal of ECT, 2007, 23, 265-273.	0.6	53
76	Visualization of Subthalamic Nuclei with Cortex Attenuated Inversion Recovery MR Imaging. NeuroImage, 2000, 11, 341-346.	4.2	52
77	Morphology of the lateral superior temporal gyrus in neuroleptic naıÌ^ve patients with schizophrenia: relationship to symptoms. Schizophrenia Research, 2003, 60, 173-181.	2.0	52
78	From Finite Element Meshes to Clouds of Points: A Review of Methods for Generation of Computational Biomechanics Models for Patient-Specific Applications. Annals of Biomedical Engineering, 2016, 44, 3-15.	2.5	52
79	Cortical volume abnormalities in posttraumatic stress disorder: an ENIGMA-psychiatric genomics consortium PTSD workgroup mega-analysis. Molecular Psychiatry, 2021, 26, 4331-4343.	7.9	52
80	Hippocampal volume deficits and shape deformities in young biological relatives of schizophrenia probands. Neurolmage, 2010, 49, 3385-3393.	4.2	51
81	Imaging aspirin effect on macrophages in the wall of human cerebral aneurysms using ferumoxytol-enhanced MRI: Preliminary results. Journal of Neuroradiology, 2013, 40, 187-191.	1.1	50
82	Diffusion weighted imaging of prefrontal cortex in prodromal huntington's disease. Human Brain Mapping, 2014, 35, 1562-1573.	3.6	49
83	Validating a new methodology for optical probe design and image registration in fNIRS studies. NeuroImage, 2015, 106, 86-100.	4.2	48
84	Impaired sensory processing measured by functional MRI in Bipolar disorder manic and depressed mood states. Brain Imaging and Behavior, 2018, 12, 837-847.	2.1	47
85	Radiation-induced Changes in MR Signal Intensity and Contrast Enhancement of Lumbosacral Vertebrae: Do Changes Occur Only Inside the Radiation Therapy Field?. Radiology, 2002, 222, 179-183.	7.3	46
86	Magnetic resonance imaging correlates of set shifting. Journal of the International Neuropsychological Society, 2007, 13, 386-92.	1.8	46
87	Effects of smoking marijuana on focal attention and brain blood flow. Human Psychopharmacology, 2007, 22, 135-148.	1.5	46
88	Antipsychotic dose and diminished neural modulation: A multi-site fMRI study. Progress in Neuro-Psychopharmacology and Biological Psychiatry, 2011, 35, 473-482.	4.8	46
89	Accelerated wholeâ€brain multiâ€parameter mapping using blind compressed sensing. Magnetic Resonance in Medicine, 2016, 75, 1175-1186.	3.0	46
90	Prefrontal cortex white matter tracts in prodromal <scp>H</scp> untington disease. Human Brain Mapping, 2015, 36, 3717-3732.	3.6	45

#	Article	IF	CITATIONS
91	Acceleration of high angular and spatial resolution diffusion imaging using compressed sensing with multichannel spiral data. Magnetic Resonance in Medicine, 2015, 73, 126-138.	3.0	45
92	Longitudinal diffusion changes in prodromal and early <scp>HD</scp> : Evidence of whiteâ€matter tract deterioration. Human Brain Mapping, 2017, 38, 1460-1477.	3.6	45
93	Brain structure in juvenile-onset Huntington disease. Neurology, 2019, 92, e1939-e1947.	1.1	45
94	Temporal pole morphology and psychopathology in males with schizophrenia. Psychiatry Research - Neuroimaging, 2004, 132, 107-115.	1.8	43
95	Quantitative Measurement of Cortical Surface Features in Localization-Related Temporal Lobe Epilepsy Neuropsychology, 2004, 18, 729-737.	1.3	43
96	Investigating connectivity between the cerebellum and thalamus in schizophrenia using diffusion tensor tractography: A pilot study. Psychiatry Research - Neuroimaging, 2008, 163, 193-200.	1.8	43
97	3-Dimensional Magnetic Resonance Spectroscopic Imaging at 3ÂTesla for Early Response Assessment of Glioblastoma Patients During External Beam Radiation Therapy. International Journal of Radiation Oncology Biology Physics, 2014, 90, 181-189.	0.8	43
98	Diffusion Tensor Imaging in Preclinical Huntington's Disease. Brain Imaging and Behavior, 2009, 3, 77-84.	2.1	41
99	Sexâ€specific effects of the Huntington gene on normal neurodevelopment. Journal of Neuroscience Research, 2017, 95, 398-408.	2.9	41
100	Abnormal development of cerebellar-striatal circuitry in Huntington disease. Neurology, 2020, 94, e1908-e1915.	1.1	41
101	Negative Symptoms in Temporal Lobe Epilepsy. American Journal of Psychiatry, 2002, 159, 644-651.	7.2	39
102	Multi-site characterization of an fMRI working memory paradigm: Reliability of activation indices. NeuroImage, 2010, 53, 119-131.	4.2	39
103	Altered brain function, structure, and developmental trajectory in children born late preterm. Pediatric Research, 2016, 80, 197-203.	2.3	39
104	Mapping effective connectivity in the human brain with concurrent intracranial electrical stimulation and BOLD-fMRI. Journal of Neuroscience Methods, 2017, 277, 101-112.	2.5	39
105	Whole-Brain Connectivity in a Large Study of Huntington's Disease Gene Mutation Carriers and Healthy Controls. Brain Connectivity, 2018, 8, 166-178.	1.7	39
106	Efficient parallel reconstruction for high resolution multishot spiral diffusion data with low rank constraint. Magnetic Resonance in Medicine, 2017, 77, 1359-1366.	3.0	37
107	Globus pallidus volume is related to symptom severity in neuroleptic naive patients with schizophrenia. Schizophrenia Research, 2005, 73, 229-233.	2.0	36
108	Spatial Characteristics of White Matter Abnormalities in Schizophrenia. Schizophrenia Bulletin, 2013, 39, 1077-1086.	4.3	36

#	Article	IF	CITATIONS
109	Reliability and reproducibility of brain tissue volumetry from segmented MR scans. European Archives of Psychiatry and Clinical Neuroscience, 2001, 251, 255-261.	3.2	35
110	The power-proportion method for intracranial volume correction in volumetric imaging analysis. Frontiers in Neuroscience, 2014, 8, 356.	2.8	35
111	Effect of Trinucleotide Repeats in the Huntington's Gene on Intelligence. EBioMedicine, 2018, 31, 47-53.	6.1	34
112	Subcortical, cerebellar, and magnetic resonance based consistent brain image registration. NeuroImage, 2003, 19, 233-245.	4.2	33
113	Alterations of the cerebellum and basal ganglia in bipolar disorder mood states detected by quantitative T1ϕmapping. Bipolar Disorders, 2018, 20, 381-390.	1.9	33
114	Putting race in context: social class modulates processing of race in the ventromedial prefrontal cortex and amygdala. Social Cognitive and Affective Neuroscience, 2017, 12, 1314-1324.	3.0	32
115	Validation of phalanx bone three-dimensional surface segmentation from computed tomography images using laser scanning. Skeletal Radiology, 2007, 37, 35-42.	2.0	31
116	Toward fully automated processing of dynamic susceptibility contrast perfusion MRI for acute ischemic cerebral stroke. Computer Methods and Programs in Biomedicine, 2010, 98, 204-213.	4.7	31
117	Effects of age on white matter integrity and negative symptoms in schizophrenia. Schizophrenia Research, 2015, 161, 29-35.	2.0	31
118	Life events and hippocampal volume in first-episode major depression. Journal of Affective Disorders, 2008, 110, 241-247.	4.1	30
119	Associations of White Matter Integrity and Cortical Thickness in Patients With Schizophrenia and Healthy Controls. Schizophrenia Bulletin, 2014, 40, 665-674.	4.3	30
120	Disruption of response inhibition circuits in prodromal Huntington disease. Cortex, 2014, 58, 72-85.	2.4	30
121	Frontal hypometabolism in elderly breast cancer survivors determined by [¹⁸ F]fluorodeoxyglucose (FDG) positron emission tomography (PET): a pilot study. International Journal of Geriatric Psychiatry, 2015, 30, 587-594.	2.7	30
122	Are Anesthesia and Surgery during Infancy Associated with Decreased White Matter Integrity and Volume during Childhood?. Anesthesiology, 2017, 127, 788-799.	2.5	30
123	Age and Regional Cerebral Blood Flow in Schizophrenia. Journal of Neuropsychiatry and Clinical Neurosciences, 2002, 14, 19-24.	1.8	29
124	Long-Term Neuropsychological, Neuroanatomical, and Life Outcome in Hippocampal Amnesia. Clinical Neuropsychologist, 2012, 26, 335-369.	2.3	29
125	A Controlled Quantitative MRI Volumetric Investigation of Hippocampal Contributions to Immediate and Delayed Memory Performance. Journal of Clinical and Experimental Neuropsychology, 2003, 25, 1117-1127.	1.3	28
126	Automated hexahedral meshing of anatomic structures using deformable registration. Computer Methods in Biomechanics and Biomedical Engineering, 2009, 12, 35-43.	1.6	28

#	Article	IF	CITATIONS
127	Echo-planar FLAIR imaging in evaluation of intracranial lesions Radiographics, 1996, 16, 575-584.	3.3	27
128	Cigarette smoking and white matter microstructure in schizophrenia. Psychiatry Research - Neuroimaging, 2012, 201, 152-158.	1.8	27
129	Myelination-related genes are associated with decreased white matter integrity in schizophrenia. European Journal of Human Genetics, 2016, 24, 381-386.	2.8	27
130	Sex-specific alterations in preterm brain. Pediatric Research, 2019, 85, 55-62.	2.3	27
131	Morphometry of the Superior Temporal Plane In Schizophrenia: Relationship to Clinical Correlates. Journal of Neuropsychiatry and Clinical Neurosciences, 2004, 16, 284-294.	1.8	26
132	Donepezil Effects on Cerebral Blood Flow in Older Adults With Mild Cognitive Deficits. Journal of Neuropsychiatry and Clinical Neurosciences, 2006, 18, 178-185.	1.8	26
133	Peripheral nerve stimulation in a whole-body echo-planar imaging system. Journal of Magnetic Resonance Imaging, 1997, 7, 405-409.	3.4	25
134	Assessment of brain age in posttraumatic stress disorder: Findings from the ENIGMA PTSD and brain age working groups. Brain and Behavior, 2022, 12, e2413.	2.2	25
135	MR imaging-based volumetry in patients with early-treated phenylketonuria. American Journal of Neuroradiology, 2005, 26, 1681-5.	2.4	24
136	The Emerging Role of Ferumoxytol-Enhanced MRI in the Management of Cerebrovascular Lesions. Molecules, 2013, 18, 9670-9683.	3.8	23
137	Brain Structural Features of Myotonic Dystrophy Type 1 and their Relationship with CTG Repeats. Journal of Neuromuscular Diseases, 2019, 6, 321-332.	2.6	23
138	MRI Tissue Classification Using High-Resolution Bayesian Hidden Markov Normal Mixture Models. Journal of the American Statistical Association, 2012, 107, 102-119.	3.1	21
139	The Relationship Between Brain Structure and Cognition in Transfused Preterm Children at School Age. Developmental Neuropsychology, 2014, 39, 226-232.	1.4	21
140	Stable Atlas-based Mapped Prior (STAMP) machine-learning segmentation for multicenter large-scale MRI data. Magnetic Resonance Imaging, 2014, 32, 832-844.	1.8	21
141	Semi-automated Phalanx Bone Segmentation Using the Expectation Maximization Algorithm. Journal of Digital Imaging, 2009, 22, 483-491.	2.9	20
142	Global Cerebral Blood Flow in Relation to Cognitive Performance and Reserve in Subjects with Mild Memory Deficits. Molecular Imaging and Biology, 2006, 8, 363-372.	2.6	19
143	Sex-specific variation of MRI-based cortical morphometry in adult healthy volunteers: The effect on cognitive functioning. Progress in Neuro-Psychopharmacology and Biological Psychiatry, 2011, 35, 616-623.	4.8	19
144	Functional T1ϕImaging in Panic Disorder. Biological Psychiatry, 2014, 75, 884-891.	1.3	19

#	Article	IF	CITATIONS
145	Precisionâ€guided sampling schedules for efficient T1ï•mapping. Journal of Magnetic Resonance Imaging, 2015, 41, 242-250.	3.4	19
146	Improved MUSSELS reconstruction for highâ€resolution multiâ€shot diffusion weighted imaging. Magnetic Resonance in Medicine, 2020, 83, 2253-2263.	3.0	19
147	qModeL: A plugâ€endâ€play modelâ€based reconstruction for highly accelerated multiâ€shot diffusion MRI using learned priors. Magnetic Resonance in Medicine, 2021, 86, 835-851.	3.0	19
148	Molecular Imaging of Cerebrovascular Lesions. Translational Stroke Research, 2014, 5, 260-268.	4.2	18
149	Neural Sensitivity to Absolute and Relative Anticipated Reward in Adolescents. PLoS ONE, 2013, 8, e58708.	2.5	18
150	Manual and automated measurement of the whole thalamus and mediodorsal nucleus using magnetic resonance imaging. Neurolmage, 2002, 17, 631-42.	4.2	18
151	Inter- and intraoperator reliability of brain tissue measures using magnetic resonance imaging. European Archives of Psychiatry and Clinical Neuroscience, 2003, 253, 301-306.	3.2	17
152	Quantitative T1ï•mapping links the cerebellum and lithium use in bipolar disorder. Molecular Psychiatry, 2015, 20, 149-149.	7.9	17
153	Cystitis-induced bladder pain is Toll-like receptor 4 dependent in a transgenic autoimmune cystitis murine model: a MAPP Research Network animal study. American Journal of Physiology - Renal Physiology, 2019, 317, F90-F98.	2.7	17
154	A pilot to assess target engagement of terazosin in Parkinson's disease. Parkinsonism and Related Disorders, 2022, 94, 79-83.	2.2	17
155	Automated bony region identification using artificial neural networks: reliability and validation measurements. Skeletal Radiology, 2008, 37, 313-319.	2.0	16
156	Abnormal Cerebellar Structure Is Dependent on Phenotype of Isolated Cleft of the Lip and/or Palate. Cerebellum, 2013, 12, 236-244.	2.5	16
157	T1ϕimaging in premanifest Huntington disease reveals changes associated with disease progression. Movement Disorders, 2015, 30, 1107-1114.	3.9	16
158	Increased contrast enhancement of the parent vessel of unruptured intracranial aneurysms in 7T MR imaging. Journal of NeuroInterventional Surgery, 2020, 12, 1018-1022.	3.3	16
159	The functional brain networks that underlie visual working memory in the first two years of life. NeuroImage, 2020, 219, 116971.	4.2	16
160	Semiautomated 3D mapping of aneurysmal wall enhancement with 7T-MRI. Scientific Reports, 2021, 11, 18344.	3.3	16
161	Modulating perceptual complexity and load reveals degradation of the visual working memory network in ageing. Neurolmage, 2017, 157, 464-475.	4.2	15
162	Detection of microbleeds associated with sentinel headache using MRI quantitative susceptibility mapping: pilot study. Journal of Neurosurgery, 2019, 130, 1391-1397.	1.6	15

#	Article	IF	CITATIONS
163	Processing pipeline for image reconstructed fNIRS analysis using both MRI templates and individual anatomy. Neurophotonics, 2021, 8, 025010.	3.3	15
164	SMS MUSSELS: A navigatorâ€free reconstruction for simultaneous multiâ€sliceâ€accelerated multiâ€shot diffusion weighted imaging. Magnetic Resonance in Medicine, 2020, 83, 154-169.	3.0	14
165	Magnetic resonance imaging (MRI) of pharmacological ascorbate-induced iron redox state as a biomarker in subjects undergoing radio-chemotherapy. Redox Biology, 2021, 38, 101804.	9.0	14
166	Measurement of in vivo spinal cord displacement and strain fields of healthy and myelopathic cervical spinal cord. Journal of Neurosurgery: Spine, 2019, 31, 53-59.	1.7	14
167	68 Usefulness of tumor volumetry by magnetic resonance (MR) imaging in assessing response to radiation therapy in carcinoma of the uterine cervix. International Journal of Radiation Oncology Biology Physics, 1995, 32, 175.	0.8	13
168	Color Enhancement of Multispectral MR Images: Improving the Visualization of Subcortical Structures. Journal of Computer Assisted Tomography, 2001, 25, 942-949.	0.9	13
169	Automated parcellation of the brain surface generated from magnetic resonance images. Frontiers in Neuroinformatics, 2013, 7, 23.	2.5	13
170	Response control networks are selectively modulated by attention to rare events and memory load regardless of the need for inhibition. NeuroImage, 2015, 120, 331-344.	4.2	13
171	EM Segmentation of the Distal Femur and Proximal Tibia: A High-Throughput Approach to Anatomic Surface Generation. Annals of Biomedical Engineering, 2011, 39, 1555-1562.	2.5	12
172	Fast iterative algorithm for the reconstruction of multishot nonâ€cartesian diffusion data. Magnetic Resonance in Medicine, 2015, 74, 1086-1094.	3.0	12
173	Cardiorespiratory fitness and hippocampal volume predict faster episodic associative learning in older adults. Hippocampus, 2020, 30, 143-155.	1.9	12
174	Eccentricity Mapping of the Human Visual Cortex to Evaluate Temporal Dynamics of Functional <i>T</i> ₁₁ Mapping. Journal of Cerebral Blood Flow and Metabolism, 2015, 35, 1213-1219.	4.3	11
175	Comprehensive reconstruction of multi-shot multi-channel diffusion data using mussels. , 2016, 2016, 1107-1110.		11
176	Recovery of Damped Exponentials Using Structured Low Rank Matrix Completion. IEEE Transactions on Medical Imaging, 2017, 36, 2087-2098.	8.9	11
177	Long-term outcome of brain structure in female preterm infants: possible associations of liberal versus restrictive red blood cell transfusions. Journal of Maternal-Fetal and Neonatal Medicine, 2021, 34, 3292-3299.	1.5	11
178	Natural bladder filling alters resting brain function at multiple spatial scales: a proof-of-concept MAPP Network Neuroimaging Study. Scientific Reports, 2020, 10, 19901.	3.3	11
179	2094 Can combined volume and perfusion analysis improve the prediction of tumor control in cervical cancer?. International Journal of Radiation Oncology Biology Physics, 1996, 36, 323.	0.8	10
180	Characterizing white matter health and organization in atherosclerotic vascular disease: A diffusion tensor imaging study. Psychiatry Research - Neuroimaging, 2013, 214, 389-394.	1.8	10

#	Article	IF	CITATIONS
181	White matter fractional anisotropy is inversely related to anxious symptoms in older adults with atherosclerosis. International Journal of Geriatric Psychiatry, 2013, 28, 1069-1076.	2.7	10
182	R1Ï•sensitivity to pH and other compounds at clinically accessible spinâ€lock fields in the presence of proteins. NMR in Biomedicine, 2020, 33, e4217.	2.8	10
183	Proton Magnetic Resonance Spectroscopy in adult cancer patients with delirium. Psychiatry Research - Neuroimaging, 2011, 191, 128-132.	1.8	9
184	Relationship altered between functional T1ï•and <scp>BOLD</scp> signals in bipolar disorder. Brain and Behavior, 2017, 7, e00802.	2.2	9
185	A general algorithm for compensation of trajectory errors: Application to radial imaging. Magnetic Resonance in Medicine, 2018, 80, 1605-1613.	3.0	9
186	New Applications of the Verdict Library for Standardized Mesh Verification Pre, Post, and End-to-End Processing. , 2008, , 535-552.		9
187	Assessment of Blood Flow in Solid Tumors Using PET. Molecular Imaging and Biology, 1998, 1, 117-121.	0.3	8
188	Evaluation of activity-dependent functional pH and T1ï•response in the visual cortex. NeuroImage, 2014, 95, 336-343.	4.2	8
189	Threeâ€Dimensional GRE T _{1ï} mapping of the brain using tailored variable flipâ€angle scheduling. Magnetic Resonance in Medicine, 2020, 84, 1235-1249.	3.0	8
190	Distinct patterns of altered quantitative T1ï•and functional BOLD response associated with history of suicide attempts in bipolar disorder. Brain Imaging and Behavior, 2021, , 1.	2.1	8
191	Metabolic abnormalities in the basal ganglia and cerebellum in bipolar disorder: A multi-modal MR study. Journal of Affective Disorders, 2022, 301, 390-399.	4.1	8
192	Compliance with medication but not structural MRI measures predict functional outcome in first-episode schizophrenia patientsâ~†. Schizophrenia Research, 2007, 90, 355-356.	2.0	7
193	Toward the Development of Virtual Surgical Tools to Aid Orthopaedic FE Analyses. Eurasip Journal on Advances in Signal Processing, 2009, 2010, 1902931-1902937.	1.7	7
194	The LURN Research Network Neuroimaging and Sensory Testing (NIST) Study: Design, protocols, and operations. Contemporary Clinical Trials, 2018, 74, 76-87.	1.8	7
195	Preliminary evaluation of pre-speech and neurodevelopmental measures in 7–11-week-old infants with isolated oral clefts. Pediatric Research, 2021, 89, 85-90.	2.3	7
196	An Analytical Framework for Quadrilateral Surface Mesh Improvement with an Underlying Triangulated Surface Definition. , 2010, , 85-102.		7
197	Electromyographic study of postural adaptation during mandibular advancement. Computer Methods in Biomechanics and Biomedical Engineering, 2009, 12, 35-37.	1.6	6
198	Surgically oriented measurements for three-dimensional characterization of tunnel placement in anterior cruciate ligament reconstruction. Computer Aided Surgery, 2012, 17, 221-231.	1.8	6

#	Article	IF	CITATIONS
199	Rapid acquisition strategy for functional T1ϕmapping of the brain. Magnetic Resonance Imaging, 2014, 32, 1067-1077.	1.8	6
200	Depressive symptoms related to low fractional anisotropy of white matter underlying the right ventral anterior cingulate in older adults with atherosclerotic vascular disease. Frontiers in Human Neuroscience, 2015, 9, 408.	2.0	6
201	Early Phase PIBâ€PET as a Surrogate for Global and Regional Cerebral Blood Flow Measures. Journal of Neuroimaging, 2019, 29, 85-96.	2.0	6
202	Fourth Ventricle Enlargement in Chiari Malformation Type I. World Neurosurgery, 2020, 133, e259-e266.	1.3	6
203	Proton Exchange Magnetic Resonance Imaging: Current and Future Applications in Psychiatric Research. Frontiers in Psychiatry, 2020, 11, 532606.	2.6	6
204	How do neural processes give rise to cognition? Simultaneously predicting brain and behavior with a dynamic model of visual working memory Psychological Review, 2021, 128, 362-395.	3.8	6
205	White matter microstructure relates to motor outcomes in myotonic dystrophy type 1 independently of disease duration and genetic burden. Scientific Reports, 2021, 11, 4886.	3.3	6
206	Mild Cognitive Impairment as an Early Landmark in Huntington's Disease. Frontiers in Neurology, 2021, 12, 678652.	2.4	6
207	Posttraumatic stress and alcohol use among veterans: Amygdala and anterior cingulate activation to emotional cues Psychology of Addictive Behaviors, 2016, 30, 720-732.	2.1	6
208	Subcortical T1-Rho MRI Abnormalities in Juvenile-Onset Huntington's Disease. Brain Sciences, 2020, 10, 533.	2.3	5
209	Neurocognitive Features of Motor Premanifest Individuals With Myotonic Dystrophy Type 1. Neurology: Genetics, 2021, 7, e577.	1.9	5
210	Multiâ€band―and inâ€planeâ€accelerated diffusion MRI enabled by modelâ€based deep learning in qâ€space a extension to learning in the spherical harmonic domain. Magnetic Resonance in Medicine, 2022, 87, 1799-1815.	nd its 3.0	5
211	Topographical Analysis of Aneurysm Wall Enhancement With 3â€Dimensional Mapping. , 2022, 2, .		5
212	Automated brain segmentation using neural networks. , 2006, , .		4
213	CT-measured lung air-trapping is associated with higher carotid artery stiffness in individuals with chronic obstructive pulmonary disease. Journal of Applied Physiology, 2018, 125, 1760-1766.	2.5	4
214	Lifetime Physical Activity and White Matter Hyperintensities in Cognitively Intact Adults. Nursing Research, 2019, 68, 210-217.	1.7	4
215	Comparison of T ₁ Rho MRI, Glucose Metabolism, and Amyloid Burden Across the Cognitive Spectrum: A Pilot Study. Journal of Neuropsychiatry and Clinical Neurosciences, 2020, 32, 352-361.	1.8	4
216	Quantum chemical insight into the effects of the local electron environment on T2*-based MRI. Scientific Reports, 2021, 11, 20817.	3.3	4

#	Article	IF	CITATIONS
217	Assessment of Gadobutrol Safety in Combination with Ionizing Radiation Using a Preclinical MRI-Guided Radiotherapy Model. Radiation Research, 2020, 195, 230-234.	1.5	4
218	Blood-Based Markers of Neuronal Injury in Adult-Onset Myotonic Dystrophy Type 1. Frontiers in Neurology, 2021, 12, 791065.	2.4	4
219	Evaluation of Older Persons with Mild Cognitive Deficits: Potential Utility of Magnetic Resonance Imaging. Annals of Clinical Psychiatry, 2008, 20, 204-208.	0.6	3
220	Hippocampal acidity and volume are differentially associated with spatial navigation in older adults. NeuroImage, 2021, 245, 118682.	4.2	3
221	la-FEMesh: anatomic FE models–a check of mesh accuracy and validity. Iowa orthopaedic journal, The, 2009, 29, 48-54.	0.5	3
222	Behavioral features in child and adolescent huntingtin geneâ€nutation carriers. Brain and Behavior, 2022, 12, .	2.2	3
223	Generating random series with known values of Kendall's tau. Computer Methods and Programs in Biomedicine, 2001, 65, 17-23.	4.7	2
224	Maximize uniformity summation heuristic (MUSH): a highly accurate simple method for intracranial delineation. , 2009, , .		2
225	Gaussian curvature analysis allows for automatic block placement in multi-block hexahedral meshing. Computer Methods in Biomechanics and Biomedical Engineering, 2011, 14, 893-904.	1.6	2
226	The effectiveness of geometry features on multi-resolution diffeomorphic demons registration in the implementation of human cortex surface parcellation. , 2011, , .		2
227	Accelerating non-Cartesian sense for large coil arrays: Application to motion compensation in multishot DWI. , 2012, , .		2
228	Hexahedral meshing of subject-specific anatomic structures using mapped building blocks. Computer Methods in Biomechanics and Biomedical Engineering, 2013, 16, 602-611.	1.6	2
229	Transportation physical activity earlier in life and areas of the brain related to dementia later in life. Journal of Transport and Health, 2021, 20, 100992.	2.2	2
230	Probing the Neural Systems Underlying Flexible Dimensional Attention. Journal of Cognitive Neuroscience, 2021, 33, 1365-1380.	2.3	2
231	Hexahedral Meshing of Subject-Specific Anatomic Structures Using Registered Building Blocks. , 2010, ,		2
232	Factors influencing daily quality assurance measurements of magnetic resonance imaging scanners. Radiological Physics and Technology, 2021, 14, 396-401.	1.9	2
233	Remodeling of the Cortical Structural Connectome in Posttraumatic Stress Disorder: Results From the ENIGMA-PGC Posttraumatic Stress Disorder Consortium. Biological Psychiatry: Cognitive Neuroscience and Neuroimaging, 2022, 7, 935-948.	1.5	2

A comparative study of diffusion tensor field transformations. , 2009, , .

#	Article	IF	CITATIONS
235	An automated pipeline for cortical surface generation and registration of the cerebral cortex. , 2011, , \cdot		1
236	Growing multiblock structures: a semi-automated approach to block placement for multiblock hexahedral meshing. Computer Methods in Biomechanics and Biomedical Engineering, 2012, 15, 1043-1052.	1.6	1
237	Preliminary Study of the Association of White-Matter Metabolite Concentrations With Disease Severity in Patients With Huntington's Disease. Journal of Neuropsychiatry and Clinical Neurosciences, 2014, 26, 101-104.	1.8	1
238	Precisionâ€guided sampling schedules for efficient T1ï•mapping. Journal of Magnetic Resonance Imaging, 2015, 41, spcone.	3.4	1
239	Population Shape Collapse in Large Deformation Registration of MR Brain Images. , 2016, , .		1
240	A Framework for Finite Element Mesh Quality Improvement and Visualization in Orthopaedic Biomechanics. , 2009, , .		1
241	Cortical Features in Child and Adolescent Carriers of Mutant Huntingtin (mHTT). Journal of Huntington's Disease, 2022, , 1-6.	1.9	1
242	Posterior Fossa Sub-Arachnoid Cysts Observed in Patients with Bipolar Disorder: a Retrospective Cohort Study. Cerebellum, 2022, , .	2.5	1
243	Quantification of blood flow using phase contrast magnetic resonance imaging. , 1995, , .		Ο
244	Improved method for correction of systematic bias introduced by the sub-voxel image registration process in functional magnetic resonance imaging (fMRI). , 2006, , .		0
245	Automated image segmentation using support vector machines. , 2007, , .		Ο
246	Partial volume correction of magnetic resonance spectroscopic imaging. , 2007, , .		0
247	Evaluation of topology correction methods for the generation of the cortical surface. Proceedings of SPIE, 2009, , .	0.8	Ο
248	White matter degeneration in schizophrenia: a comparative diffusion tensor analysis. Proceedings of SPIE, 2010, , .	0.8	0
249	Automated tissue classification of pediatric brains from magnetic resonance images using age-specific atlases. , 2016, , .		Ο
250	In Reply. Anesthesiology, 2018, 128, 1261-1261.	2.5	0
251	Semi-Automated Patient Specific Hexahedral Mesh Generation of Articular Cartilage. , 2009, , .		0
252	Automated Building Block Assignments for Finite Element Mesh Development of Patient-Specific Orthopaedic Models. , 2009, , .		0

#	Article	IF	CITATIONS
253	A Comparison of Two Automated Block Placement Methods for Multi-Block Hexahedral Finite Element Meshing. , 2010, , .		0
254	Elevated Aortic Stiffness is Associated with Lower Brain pH and Executive Function Performance in Middleâ€aged and Older Adults. FASEB Journal, 2019, 33, 696.15.	0.5	0
255	Comparison of Displacement-Based and Force-Based Mapped Meshing. , 2008, 2008, 629.		0
256	Moderate Intensity Exercise in Pre-manifest Huntington's Disease: Results of a 6 months Trial , 2021, 2, 6-36.		0